Eur. Phys. J. B **48**, 37–40 (2005)
DOI: 10.1140/epjb/e2005-00371-4

THE EUROPEAN PHYSICAL JOURNAL B

Magnetotransport properties of nano-constriction array in $La_{0.67}Sr_{0.33}MnO_3$ film

H.J. Liu[1,a], T. Yang[1], W.C. Goh[1], C.H. Sow[1], S.N. Piramanayagam[2], and C.K. Ong[1]

[1] Centre for Superconducting and Magnetic Materials, Department of Physics, National University of Singapore, 2 Science Drive 3, Singapore 117542, Singapore
[2] Data Storage Institute, 5 Engineering Drive 1, DSI Building, Singapore 117608, Singapore

Received 14 May 2005
Published online 9 December 2005 –

Abstract. Nano-constriction array in $La_{0.67}Sr_{0.33}MnO_3$ film was fabricated by using ion beam etching masked by a monolayer of packed and ordered array of SiO_2 microspheres. Nano-constrictions of around 50 nm in width were fabricated. The low field magnetoresistance (LFMR) exhibited in the samples were observed to be current dependent and the I-V characteristics of the film were found to be nonlinear. These observations were attributed to the co-existence of the ferromagnetic regions and the nano-constricted region of weakened ferromagnetic coupling where Mn^{3+}-O-Mn^{4+} bond were distorted due to the ion beam bombardment. The spin polarized bias current would strengthen local ferromagnetic coupling when passing through this nano-constricted regions. This current effect is relatively large comparing to the external magnetic field to the drop of resistance.

PACS. 75.47.Lx Manganites – 73.63.Rt Nanoscale contacts

1 Introduction

The half-metallic perovskite magnet showing colossal magnetoresistance (CMR) has been a topic of intense research in the last decade [1–3]. However, the CMR effect is only appreciable in large magnetic fields of several Tesla and it is too high for most applications. Therefore, in recent years, intense research activity has been focused on the extrinsic low field magnetoresistance (LFMR) of various structures such as grain boundary junctions [4–6], magnetic tunneling junctions [7], nano-constrictions [8–10] etc. Very large magnetoresistances have been achieved in these structures and they were found to be current dependent. Several models have been proposed to explain the current dependence of the magnetotransport properties [5,9,11], however, consensus has not been reached. In this work we aim to further our study on magnetotransport properties of the nano-constriction array in $La_{0.67}Sr_{0.33}MnO_3$ (LSMO) film and to shed further light on its origin of nonlinear I-V characteristics. In the previous study [10], nano-constriction was fabricated in the pre-patterned microbridge masked by a monolayer of colloidal microspheres by ion beam etching. However, in the present study, a microbridge was patterned after the ion beam etching process in a region that was more uniformly covered with nano-constrictions, which allows us to have more control on the dimension of nano-constriction to obtain more homogeneous samples. Furthermore, the transport measurement of the nano-constriction array was carried out before and after annealing to ensure that our observations are contributed from the oxygen-deficient state in nano-constrictions caused by ion beam bombardment. We also found that the spin polarized bias current has effect of strengthening local magnetic coupling when passing through the oxygen-deficient nano-constriction.

2 Experimental details

Epitaxial thin films of LSMO were grown on STO [100] substrate from a stoichiometric target by pulsed laser deposition (PLD) with KrF laser of $\lambda = 248$ nm. The deposition conditions were a substrate temperature of 750 °C in an oxygen partial pressure of 0.3 mbar. The laser energy density per pulse was about 1.5 Jcm^{-2} and the pulse repetition rate was 5 Hz. Then the deposited films were annealed at 750 °C under oxygen pressure of 1 atm for 1 h. The film thickness was determined to be about 200 nm with a step profiler.

After thin film deposition, a drop of the solution from commercially purchased aqueous suspension of SiO_2 microspheres [Duke Scientific Corp.] with a diameter of 0.99 ± 0.05 μm was dropped onto the oxide films. These microspheres self-assembled into a nearly hexagonally closed-packed ordered configuration that served as a mask for ion beam etching. The LSMO films partially covered by packed microspheres were then placed inside the chamber of an ion beam etching facility equipped with RF 25 ion source [Oxford Applied Research]. The working gas was Ar. The RF power used was 350 W and the accelerating

[a] e-mail: g0306128@nus.edu.sg

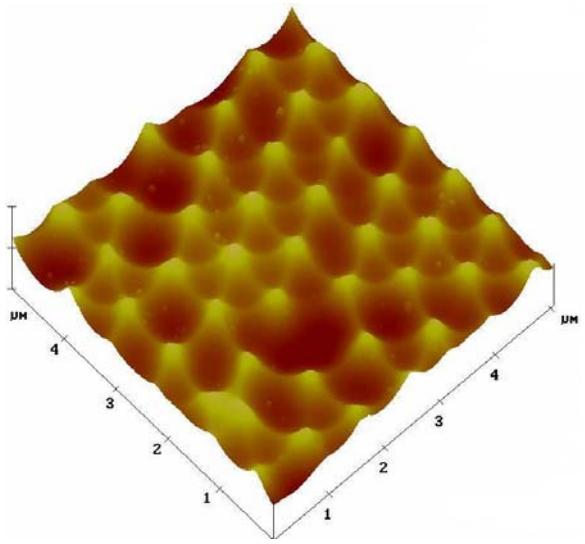

Fig. 1. AFM image of nano-constriction array on LSMO film after ion beam etching for 60 min. The brighter regions are the residual LSMO film. Nano-constrictions of around 50 nm in width are fabricated in LSMO film.

voltage was 600 V. The duration of the etching process was 60 min.

Figure 1 shows an AFM picture of the nano-constriction array formed on the LSMO film after the whole process. The parts of the film which were not covered by the mask were etched away and the area shielded by the spheres remained. The nano-constrictions about 50 nm were formed on the contact point between two spheres. It is found that the remained islands connected by nano-constrictions are pyramid-liked. This is because as a mask, the SiO_2 spheres shrank at the process of ion beam etching and the area shielded by microspheres became smaller with the etching time.

After etching, the microspheres were removed and a bridge of 20 μm in width and 50 μm in length was patterned on the etched area using conventional wet etching technique. Figure 2 shows the schematics of the whole process of sample preparation. After sample fabrication, four-point probe method was used to measure the magnetotransport properties of the bridge with magnetic field up to 3000 Gauss applied parallel to the current.

3 Results and discussions

Biased at the current of 1 μA, the temperature dependence of the resistance with external magnetic field of 3000 Gauss and that without external field are shown in Figure 3. The *R-T* curve of the original continuous LSMO film is also presented as an inset in Figure 3, which shows the metallic behavior. The resistance of the nano-constriction-patterned thin film had increased by several orders of magnitude after being etched and the metal-insulator transition temperature T_P shifted from above 300 K to about 170 K. For the nano-constriction-patterned sample, when temperature is below T_P, the gap between

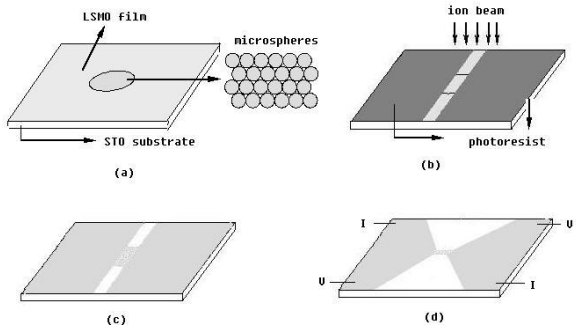

Fig. 2. Schematics of the sample preparing process. (a) deposition of a monolayer of SiO_2 microspheres onto the center of the LSMO film (b) the top view of the film covered by photoresist except a strip at the center of the film and subjected to ion beam (c) after the ion beam etching, the photoresist has been cleared and the microspheres have been removed (d) a microbridge is fabricated on the etched area for transport measurement.

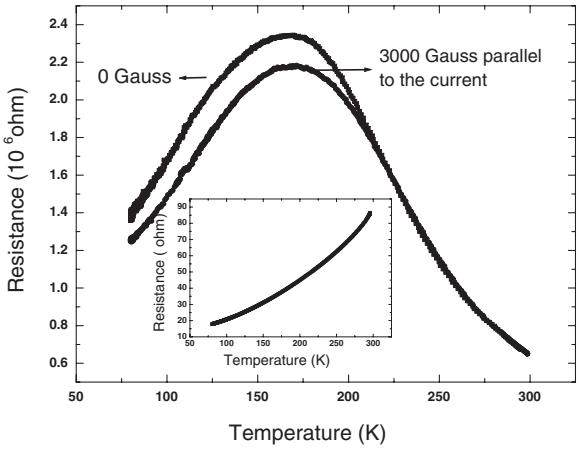

Fig. 3. *R-T* curves of film with bias current of 1 μA after being etched for 60 min. The two curves represent the measurements carried out with and without applied field of 3000 Gauss respectively. Insets: *R-T* curve of the original film where T_P is above 300 K with resistance much smaller than the etched film by several orders of magnitude.

the *R-T* curve with applied magnetic field of 3000 Gauss and that without magnetic field is almost a constant. Therefore, the MR ratios of the film increase as the temperature decreases. This behavior is very similar to those in the polycrystalline bulk materials or thin film. However, further investigation on the temperature dependence of the resistance of nano-constriction array with bias current from 10 nA to 1 μA under zero magnetic field revealed that (Fig. 4) the value of peak resistance became smaller and the T_P shifted to a higher temperature when the bias current increased. Here we could rule out the thermal effect as it would cause T_P to shift to a lower temperature, which is contrary to the observations for our sample. So far no such phenomenon was reported in the polycrystalline bulk materials or continuous thin films.

Furthermore, Figure 5 shows the *I-V* curves at different temperature without magnetic field for

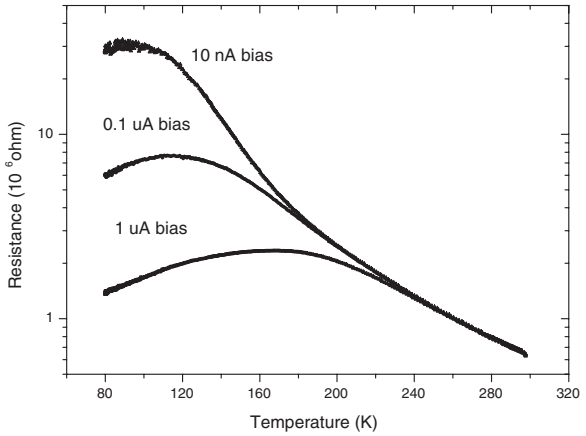

Fig. 4. Temperature dependence of the resistance of nano-constriction array with bias current form 10 nA to 1 μA under zero-field. The peak resistance became smaller and the T_P shifted to a higher temperature when the bias current was increased.

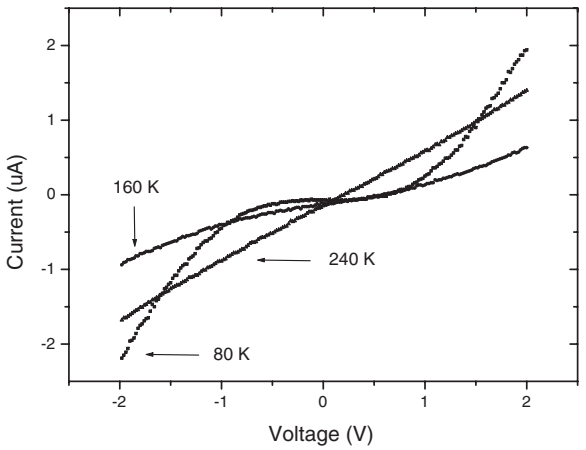

Fig. 5. I-V characteristic of the nano-constriction array under different temperature without applied field. This nano-constriction array has stronger nonlinear I-V characteristic at low temperature.

the nano-constriction-patterned sample. This nano-constriction array has stronger nonlinear I-V characteristic at low temperature and the nonlinearity becomes less apparent with the temperature increasing. The nonlinear I-V characteristic have been observed in our previous studies [10] and other structures such as grain boundary junctions [4–6], magnetic tunnelling junctions [7], nano-constrictions [8–10] etc. There are several proposals to explain the current dependence of the magnetotransport properties [5,9,11]. Below, we shall discuss the contribution of ion beam radiation to the oxygen deficiency in the film and its effect to the nonlinear transport behavior.

A magnetoresistance measurement was carried out on the sample before and after the ion beam etching at 80 K. No significant MR ratio was observed before the film was etched with the applied field up to 3000 Gauss. After ion beam etching, the low field MR increased significantly. Further study found that this LFMR was current dependent, as shown in Figure 6. Although the noise increased with decreasing bias current, it is apparent that the MR ratio increased with decreasing bias current. When the bias current was at 10 nA, the nano-constriction array exhibited about 30% MR ratio with applied field up to 3000 Gauss.

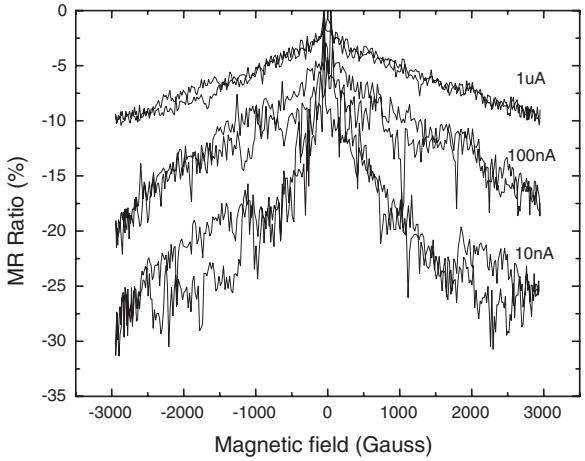

Fig. 6. Current dependence of MR ratio of the nano-constriction array at 80 K. The MR ratio increased with decreasing bias current.

In the course of the sample fabrication, it is inevitable that there will be some oxygen deficiency in the film due to the ion bombardment. Since the energy of the ion beam of 600 eV is very low, it is expected that the influence of oxygen deficiency is significant only at the area of the nano-constrictions where the thickness is much thinner than that of the islands (see Fig. 1). Other than the constriction region, there is almost no change of oxygen content in the film except for a very thin layer of surface comparing to original film. Since the oxygen deficiency will cause the reduction of hole concentration and the change of Mn-O-Mn bond angle, and further decrease the Curie temperature [12,13], the patterned film can be viewed as a system in which the ferromagnetic islands were connected by nano-constrictions with weakened magnetic coupling. In terms of the double exchange interaction [14], the metal-insulator transition temperature is expected to shift to a low temperature since the current has to flow through the nano-constriction where the magnetic coupling is weakened, as show in Figure 3. Spin polarized current flowing through regions of weakened magnetic coupling will exhibit low field MR as shown in Figure 3, similar to that attributed to the grain boundary. These are consistent with the results of the ion irradiated manganites [15,16].

In order to confirm the oxygen deficient state in nano-constriction caused by ion bombardment, the sample was annealed at 750 °C under oxygen pressure of 1 atm for 1 h. And then the same measurements were repeated. Through annealing in oxygen atmosphere, the constriction absorbed oxygen and the resistance of the sample decreased significantly. The R-T curve (not shown here) indicated that the metal-insulator transition temperature T_P shifted back to a temperature higher than 300 K. No

nonlinear phenomenon was observed in I-V characteristic and magnetotransport measurements even at low temperature.

The current dependence of T_P, shown in Figure 4, strongly indicated that there is a relationship between magnetic properties of the nano-constriction array and the current flowing through it in terms of double exchange interaction. Westerberg et al. [17] proposed a model to explain a dependence of the hysteretic low field MR on the bias current. The model is based on an assumption that a polarized charge carrier from the ferromagnetic region due to double exchange will strengthen local magnetic coupling in the region of weakened ferromagnetic coupling during its transition. This is plausible if the time interval for each manganese ion encountering two successive spin-polarized electrons ($10^{-7} \sim 10^{-9}$ s in this experiment) is comparable to or even smaller than the spin relaxation time ($>10^{-8}$ s [18]). This current effect is relatively large when comparing with the effect of external magnetic field. (see Figs. 4 and 6) At 80 K, increasing the bias current from 10 nA to 0.1 μA will cause the resistance drop of 79.3% and to 1 μA will cause the resistance drop of 94.8%, which are much larger than the magnetoresistance of about 30% at 10 nA bias current with magnetic field up to 3000 Gauss. This suggests that the effect of a bias current of as small as 0.1 μA to the resistance drop is equivalent to the application of an external field much larger than 3000 gauss on the system.

Based on the assumption described above, the increase of the bias current caused more polarized charge carriers pass through the weakly coupled nano-constrictions hence creating a stronger ferromagnetic coupling between the spin-polarized islands resulting in a higher Curie temperature. Therefore, with the increase of the bias current, T_P will increase and the peak resistance will decrease in the framework of double exchange interaction, as shown in Figure 4. However, at lower bias current, the applied field could more easily modify the magnetic configuration of the ferromagnetic islands because of the weaker coupling between two ferromagnetic islands and hence produce a larger MR ratio, as shown in Figure 6.

We now turn to explain the nonlinearity of the I-V characteristic exhibited by the nano-constriction array. As discussed above, in the nano-constriction array system, the value of T_P shifted to a higher temperature with increasing bias current. A maximum temperature of $(T_P)_{max}$ was expected. For a temperature higher than $(T_P)_{max}$, the nano-constriction array will be in paramagnetic insulating state and its resistance will be a constant no matter how large the bias current is. Thus the I-V curve will be linear, as shown in Figure 5 for the case of measurement at 240 K. For a temperature below the $(T_P)_{max}$, at a very small applied current, the nano-constrictions are in paramagnetic and insulating state due to very weak ferromagnetic coupling. With the increase of the bias current, the nano-constrictions will gradually become ferromagnetic and conductive. The larger the bias current applied, the higher the Curie temperature of the nano-constrictions and the smaller the possibility for electrons being scattered by magnon, which leads to a smaller resistance. Hence the nano-constriction array will exhibit nonlinear I-V characteristic at a low temperature.

4 Conclusions

In conclusion, we have studied the magnetotransport properties of the nano-constriction array in $La_{0.67}Sr_{0.33}MnO_3$ film fabricated using ion beam etching masked by a monolayer of packed and ordered array of SiO_2 microspheres. Strong current dependence of the magnetotransport properties and nonlinear I-V characteristic have been observed. All these observations are attributed to the co-existence of the ferromagnetic regions and the weakened ferromagnetic coupling nano-constricted region where the Mn^{3+}-O-Mn^{4+} bond are distorted. The weakened ferromagnetic coupling is arisen from local oxygen deficiency which is contributed from ion bombardment and could be eliminated by further annealing of the sample.

References

1. S. Jin, T.H. Tiefel, M. McCormack, R.A. Fastnacht, R. Ramesh, L.H. Chen, Science **264**, 413 (1994)
2. R. von Helmolt, J. Wecker, B. Holzapfel, L. Schultz, K. Samwer, Phys. Rev. Lett. **71**, 2331 (1993)
3. J.M.D. Coey, M. Viret, S. von Molnár, Adv. Phys. **48**, 167 (1999)
4. H.Y. Hwang, S-W. Cheong, N.P. Ong, B. Batlogg, Phys. Rev. Lett. **77**, 2041 (1996)
5. M. Ziese, G. Heydon, R. Höhne, P. Esquinazi, J. Dienelt, Appl. Phys. Lett. **74**, 1481 (1999)
6. N.D. Mathur, G. Burnell, S.P. Isaac, T.J. Jackson, B.-S. Teo, J.L. MacManus-Driscoll, L.F. Cohen, J.E. Evetts, M.G. Blamire, Nature **387**, 266 (1997)
7. J.Z. Sun, A. Gupta, Annu. Rev. Mater. Sci. **28**, 45 (1998)
8. N. García, M. Muñoz, Y.-W. Zhao, Phys. Rev. Lett. **82**, 2923 (1999)
9. J.J. Versluijs, M.A. Bari, J.M.D. Coey, Phys. Rev. Lett. **87**, 026601 (2001)
10. J. Li, D.N. Zheng, X.S. Rao, C.H. Sow, L. Chen, C.K. Ong, Europhys. Lett. **65**, 823 (2004)
11. C. Höfener, J.B. Philipp, J. Klein, L. Alff, A. Marx, B. Büchner, R. Gross, Europhys. Lett. **50**, 681 (2000)
12. P.G. Radaelli, G. Iannone, M. Marezio, H.Y. Hwang, S.-W. Cheong, J.D. Jorgensen, D.N. Argyriou, Phys. Rev. B **56**, 8265 (1997)
13. J. Li, J.M. Liu, H.P. Li, H.C. Fang, C.K. Ong, J. Magn. Magn. Mater. **202**, 285 (1999)
14. C. Zener, Phys. Rev. **81**, 440 (1951)
15. C.-H. Chen, V. Talyansky, C. Kwon, M. Rajeswari, R.P. Sharma, R. Ramesh, T. Venkatesan, John Melngailis, Z. Zhang, W.K. Chu, Appl. Phys. Lett. **69**, 3089 (1996)
16. S.M. Watts, M. Li, S. Wirth, K.-H. Dahmen, S. von Molnár, P. Xiong, A. S. Katz, R.C. Dynes, J. Appl. Phys. **85**, 4791 (1999)
17. W. Westerburg, F. Martin, S. Friedrich, M. Maier, G. Jakob, J. Appl. Phys. **86**, 2173 (1999)
18. A. Shengelaya, Guo-meng Zhao, H. Keller, K.A. Müller, Phys. Rev. Lett. **77**, 5296 (1996)